Neuro-Oncology Advances
6(1), vdae187, 2024 | https://doi.org/10.1093/noajnl/vdae187 | Advance Access date 19 November 2024

Ion channel modulator DPI-201-106 significantly enhances antitumor activity of DNA damage response inhibitors in glioblastoma

Brittany Dewdney,[†] Panimaya Jeffreena Miranda,[†] Mani Kuchibhotla, Ranjith Palanisamy, Caitlyn Richworth, Carol J. Milligan, Zi Ying Ng, Lauren Ursich, Steve Petrou, Emily V. Fletcher, Roger J. Daly, Terry C.C. Lim Kam Sian, Santosh Valvi, Raelene Endersby and , Terrance G. Johns

All author affiliations are listed at the end of the article

[*]Corresponding Author: Terrance G. Johns, PhD, The Kids Research Institute, Perth, Western Australia, Australia (terrance.johns@telethonkids.org.au).

[†]These authors contributed equally as shared first authors.

Abstract

Background. Glioblastoma, a lethal high-grade glioma, has not seen improvements in clinical outcomes in nearly 30 years. Ion channels are increasingly associated with tumorigenesis, and there are hundreds of brain-penetrant drugs that inhibit ion channels, representing an untapped therapeutic resource. The aim of this exploratory drug study was to screen an ion channel drug library against patient-derived glioblastoma cells to identify new treatments for brain cancer.

Methods. Seventy-two ion channel inhibitors were screened in patient-derived glioblastoma cells, and cell viability was determined using the ViaLight Assay. Cell cycle and apoptosis analysis were determined with flow cytometry using PI and Annexin V staining, respectively. Protein and phosphoprotein expression was determined using mass spectrometry and analyzed using gene set enrichment analysis. Kaplan-Meier survival analyses were performed using intracranial xenograft models of GBM6 and WK1 cells.

Results. The voltage-gated sodium channel modulator, DPI-201-106, was revealed to reduce glioblastoma cell viability in vitro by inducing cell cycle arrest and apoptosis. Phosphoproteomics indicated that DPI-201-106 may impact DNA damage response (DDR) pathways. Combination treatment of DPI-201-106 with the CHK1 inhibitor prexasertib or the PARP inhibitor niraparib demonstrated synergistic effects in multiple patient-derived glioblastoma cells both in vitro and in intracranial xenograft mouse models, extending survival of glioblastoma-bearing mice.

Conclusions. DPI-201-106 enhances the efficacy of DDR inhibitors to reduce glioblastoma growth. As these drugs have already been clinically tested in humans, repurposing DPI-201-106 in novel combinatorial approaches will allow for rapid translation into the clinic.

Key Points

- The voltage-gated sodium channel modulator DPI-201-106 induces cell cycle arrest in brain cancer.
- DPI-201-106 works in synergy with DNA damage response inhibitors in brain tumors.

Glioblastoma, a WHO grade 4 high-grade glioma, remains a deadly diagnosis with one of the worst prognoses in clinical oncology.[1] No advances have been made to improve treatment and survival outcomes in decades, and the current standard of care (SOC) of maximal safe resection followed by radiotherapy (RT) and temozolomide (TMZ) only extends

Importance of the Study

There is broad agreement that combination therapy strategies are required to improve clinical outcomes in high-grade brain cancer. Recent preclinical data suggest that drugs that target ion channels represent an unused resource of brain-penetrant inhibitors that may be efficacious for treating brain cancer and amenable to drug repurposing. However, it is unlikely that single-agent ion channel drugs will be highly effective clinical agents. DPI-201-106, a voltage-gated sodium channel modulator, demonstrates synergistic effects with inhibitors of the DNA damage response pathway in patient-derived preclinical models of glioblastoma. Thus, we have combined 2 rational therapeutic strategies to develop a new treatment approach for glioblastoma. Given that all the drugs described here have been clinically approved or evaluated in human clinical trials, these combinations can be rapidly translated into the clinic.

survival marginally, where most patients will experience local tumor reoccurrence.[2] There is a desperate clinical need to explore all avenues for improved therapeutic strategies.

Identifying novel drug targets and developing suitable drugs that meet the unique clinical needs for treating brain tumors is both time-consuming and expensive.[3,4] Drug repurposing is a potential solution to promote faster entry into the clinic, where it may eliminate the need to conduct dose escalation studies and extensive safety profiles, saving time and money to accelerate their use in phase II/III clinical trials. Indeed, this makes drug repurposing for developing new cancer therapeutic strategies an attractive option. However, several contributing factors have prevented the clinical translation of therapeutic strategies into improved survival for glioblastoma patients. One of the major obstacles is that a large majority of anticancer-targeted therapies do not cross the blood-brain barrier (BBB), rendering them ineffective for brain cancer patients. Thus, we must make strategic considerations for investing future scientific efforts and resources when it comes to developing new strategies for brain cancer treatment.

Neural inputs play a critical role in tumorigenesis through direct interaction with glioma cells via synapse formation,[5] highlighting that brain tumor tissue is uniquely supported by electrically active neurons, simultaneously driving tumorigenicity and neuronal dysfunction. Ion channels are pore-forming proteins that reside within plasma membranes and play significant roles in neurological function and disease by regulating cellular ionic flux.[6] Due to the critical importance of ionic flux in actional potential and neuronal function, ion channels play a significant role in glioma development as they mediate the neuron/glioma cell interaction.[7] There are hundreds of ion channel genes in the human genome,[8] and the FDA has approved hundreds of drugs that target ion channels, many of which are used for the treatment of neurological conditions such as pain and epilepsy. As such, these drugs can readily cross the BBB and, therefore, represent an untapped source of drugs that may have targeted efficacy in brain cancer.[9]

Despite this therapeutic potential, the scope of using ion channel blockers as a novel targeted treatment strategy for brain cancer has yet to be explored to its full capacity. In this study, we sought to delve into these unexploited resources. Using an unbiased approach to drug repurposing and discovery, we screened patient-derived glioblastoma cancer cell lines against a library of 72 ion channel inhibitors to identify drugs with efficacy against brain cancer.

Materials and Methods

Cell Lines and Culture Conditions

Patient-derived glioblastoma cell lines (GBM6,[10] GBM39,[10] SB2, WK1, Pr1.1, GBML1, RN1, and RR2) were cultured as previously described.[11,12] GBM6 and GBM39 were cultured as spheroids in ultra-low attachment (ULA) plates and SB2 and WK1 cells were cultured as adherent monolayers on Cultrex-treated plates (Cultrex™ Basement Membrane Extract, PathClear™, R&D Systems). Cell lines were transduced to enable expression of luciferase (LUC) and green fluorescent protein (GFP) (GBM6-LUC-GFP and WK1-LUC-GFP), or a puromycin acetyltransferase/luciferase fusion protein (pacLuc2) as previously described.[11,13]The lentiviral and retroviral expression constructs used, pCL20-MSCV-ires-GFP-ires-Luc2 and MSCV-ires-pacLuc2, were kindly provided by Arthur Neinhuis and Richard Williams of St Jude Children's Research Hospital.

Cell Viability Assay

For the ion channel drug screen, ion channel drugs from the drug library (Supplementary Table 1; ENZO) were titrated between 1 nM and 10 μM concentrations and tested on the patient-derived cell lines. For GBM6 and GBM39 spheroid cells, cells were seeded as 5000 cells per well in 96-well ULA plates (Revvity, 6055330). For SB2 and WK1 adherent cells, cells were seeded as 2000 cells per well in 96-well plates. Cell viability was determined after 7 days of drug treatment using ViaLight Plus Cell Proliferation and Cytotoxicity BioAssay Kit (Lonza, LT07-221). The response for each treatment was plotted as a percentage of cell viability relative to vehicle-treated cells (DMSO). The ViaLight assay was also used to determine dose-response curves and combination matrix curves for prexasertib (HY-18174A, MedChemExpress), SOL578 (provided by Sentinel Oncology Limited), ceralasertib (HY-19323, MedChemExpress), adavosertib (HY-10993, MedChemExpress), and niraparib (HY-10619, MedChemExpress). Drug interaction analyses to

determine synergy or antagonism were performed using the SynergyFinder 3.0 package[14] in R.

Electrophysiology

Electrophysiological recording and analysis of GBM39 cells were performed as described.[15] Briefly, GBM39 whole-cell sodium currents derived from voltage-gated sodium channels were recorded using Nanion Patchliner® (Nanion Technologies). Currents were isolated and activated using standard voltage-clamp protocols.

Cell Cycle and Apoptosis Analysis

Glioblastoma cells were treated with either a vehicle control (DMSO), 10 μM of either SKF96365 or DPI-201-106, or prexasertib (25 nM for GBM6/GBM30, 100 nM for SB2, and 50 nM for WK1), alone or in combination. For cell cycle analysis, the cells were fixed in 70% ethanol and stained with FxCycle™ PI/RNase staining solution (Thermo Fisher Scientific). For apoptosis analysis, cells were stained with the FITC Annexin V apoptosis detection kit (BD Biosciences). The samples were run on a LSRFortessa X-20 (BD Biosciences) with a minimum of 10 000 events collected per sample. Data were analyzed using FlowJo Software (FlowJo).

Protein Extraction and Immunoblotting

Drug-treated cells were washed in ice-cold phosphate-buffered saline (PBS) and lysed on ice using radioimmunoprecipitation assay (RIPA) buffer (Thermo Fisher Scientific) supplemented with 2X Halt protease and Phosphatase inhibitor cocktail (Thermo Fisher Scientific), 1 mM EDTA (Thermo Fisher Scientific), and 2 mM sodium orthovanadate (Sigma Aldrich). To analyze protein expression of mitosis markers, cell cycle synchronization (cells blocked in G1) was performed using double thymidine block prior to cell lysis at 24, 48, or 72 h. The soluble protein fraction was quantified by BCA Protein Assay Kit (Thermo Fisher Scientific); 50 μg of total protein lysate was separated on 4-12% Bis-Tris gradient SDS-PAGE gels (Thermo Fisher Scientific) and transferred to polyvinylidene difluoride membranes using an iBlot 2 (Invitrogen). Membranes were blocked in Intercept blocking buffer (LI-COR) and washed with Tris-buffered saline with Tween 20 (TBST), and proteins were detected using antibodies described in Supplementary Table 2. Protein expression was quantified using an Odyssey imaging system and images were processed using Image Studio Lite Ver 5.2 software (LI-COR).

Intracranial Glioblastoma In Vivo Models

All animal experiments were approved by the Telethon Kids Institute Animal Ethics Committee and performed in accordance with the Australian Code for the Care and Use of Animals for Scientific Purposes. For orthotopic xenografts, GBM6-LUC-GFP or WK1-LUC-GFP cells were suspended in Matrigel® (BD Biosciences) (3×10^5 in 3 μL) and intracranially implanted in female Balb/c nude mice aged 6 weeks (Animal Resources Centre), as previously described.[13] Mice received water and food ad libitum along with nutritional enrichment for the entire period of the study. Animals were monitored weekly for tumor progression using the Xenogen IVIS System (Caliper Life Science). SKF96365 (in sterile isotonic saline) or DPI-201-106 (in 10% DMSO, 18% captisol) were administered 5 times per week via intraperitoneal injection at 60 mg/kg/dose. Prexasertib (20% captisol) was administered intravenously twice per week at 20 mg/kg. The dosing schedule for SKF96365 and DPI-201-106 was developed by injecting a range of doses in combination with our optimized dose of prexasertib[16] and assessing for toxicity. Niraparib (10% DMSO, 30% PEG300, 5% Tween80) was administered via oral gavage 3 times per week at 30 mg/kg. The frequency of drug administration was based on its known half-life and length of treatment based on the projected survival of the animals. Treatment duration was 4 weeks and the time to survival was monitored from the day of implantation, where animals were euthanized at ethical end point due to tumor-related morbidities.

Mass Spectrometry

WK1 cells were treated with 10 μM DPI-201-106 for 24 h and then lysed with 8 M Urea lysis buffer and subject to phosphoproteomics analysis as previously described.[17,18] The proteomics and phosphoproteomics samples were analyzed on an UltiMate 3000 RSLC nano liquid chromatography system (Thermo Fisher Scientific) coupled to a Q-Exactive HF mass spectrometer (Thermo Fisher Scientific). The mass spectrometry raw data files were then analyzed with the MaxQuant analysis software using the default parameters. Enzyme specificity was defined to Trypsin/P and LysC/P. Carbamidomethylation (C) was set as a fixed modification, whereas oxidation (M), acetyl (protein N terminus), deamidation (NQ), and phosphorylation (STY) were set as variable modifications. Statistical and differential expression analyses were conducted using the limma package in R.[19]

Bioinformatics Analysis

Bioinformatics analysis was performed on the mass spectrometry data using 3 datasets to identify differentially expressed tyrosine phosphorylated proteins ($n = 362$ phosphosites), serine/threonine phosphorylated proteins ($n = 9114$ phosphosites), and whole proteins (WPs) ($n = 5806$). Volcano plots were produced using Python (version 3.9.13), where a $-\log10(P\text{-value})$ of > 1 and log2(fold change) of either > 1 or < -1 were used to identify differentially expressed proteins. Differentially expressed proteins were imported into DAVID (Database for Annotation, Visualization, and Integrated Discovery) to generate a functional annotation chart generated from gene sets acquired from Gene Ontology Biological Processes (GOBP), Kyoto Encyclopedia of Genes and Genomes (KEGG), BioCarta, WikiPathways, and Reactome. Default settings were used for all remaining parameters. Gene sets representing

cellular biological processes and pathways were obtained from the Human Molecular Signature Database (MSigDB, version v2023.1.Hs) at the Broad Institute.[20] We searched the total gene sets to identify those related to "DNA damage" and "cell cycle" and analyzed these gene sets with Gene Set Enrichment Analysis (GSEA) in Python.

Statistical Analysis

Statistical analyses were performed using Prism 9.0 (GraphPad). All viability assays were performed in biological and technical triplicates and data were expressed as mean ± SEM. For drug interaction analyses, *P*-values were generated from the SynergyFinder R program.[21] Flow cytometry experiments were repeated 3 times, data were presented as mean ± SD, and statistical significance was determined with either a Kruskal-Wallis test or a 2-way ANOVA and Tukey's multiple comparisons test. All western blot experiments were performed in triplicate, and the statistical significance of quantified blots was determined with a 2-way ANOVA and Dunnett's multiple comparisons test. For in vivo studies, survival was assessed using Kaplan-Meier curve analyses, and significance was calculated using the log-rank Mantel-Cox test, where each treatment group was compared with the control group. To account for the 3 repeated comparisons, the Bonferroni-corrected threshold for statistical significance was set at $P < .0166667$. Values of significance are indicated by asterisks and described in each figure legend where appropriate.

Results

Identification of Ion Channel Drugs That Reduce Glioblastoma Viability In Vitro

To identify ion channel drugs that inhibit glioblastoma viability, we performed a drug screen using 72 ion channel modulators on 3 patient-derived glioblastoma cell lines (Figure 1 and Supplementary Table 1). This revealed 11 ion channel drugs that significantly reduced the viability of GBM6 cells by > 50% (Figure 1A). Validation of the drug screen was performed in GBM39 cells (Figure 1B) and SB2 cells (Figure 1C) to identify drugs that inhibited both primary and treatment-resistant recurrent glioblastoma, respectively. Based on these results, thapsigargin, flunarizine-2HCl, SKF96365, niguldipine, and DPI-201-106 were identified as drugs that inhibited all glioblastoma cell lines by at least 40%. Thapsigargin has already been evaluated in a Phase 2 trial for glioblastoma (NCT02067156) hence we did not pursue it further. To validate our screen, we further tested flunarizine-2HCl, SKF96365, niguldipine, and DPI-201-106 to determine the IC50 in GBM6, GBM39, and SB2 cells (Figure 2). For each compound, the inhibitory response was similar between the glioblastoma cell lines, with no obvious discrepancies between the primary and recurrent glioblastoma cell lines (Figure 2A-D and Supplementary Table 3). To further evaluate their anticancer effects, GBM6 cells were treated with 10 μM of either flunarizine-2HCl, SKF96365, niguldipine, or DPI-201-106, and apoptosis was examined after 7 days using Annexin V staining (Figure 2E). Treatment with 10 μM of flunarizine-2HCl, niguldipine, SKF969365, or DPI-201-106 led to > 40% of cells apoptotic after 7 days (Figure 2E). Flunarizine-2HCl has already been patented for use in glioma (KR101588949B1), so we chose not to explore this drug further. SKF96365 and niguldipine are both Ca^{2+} blockers that have been evaluated previously in glioblastoma.[22,23] The Na^{+} channel modifier, DPI-201-106, has not been tested in glioblastoma. By comparison, GBM6 cells treated with 10 μM of DPI-201-106 or SKF96365 displayed similar levels of apoptosis (Figure 2E). Therefore, we decided to conduct a detailed analysis of DPI-201-106 and 1 Ca^{2+} channel drug SKF96365. Dose-response curves for SKF96365 and DPI-201-106 were undertaken in an additional 5 patient-derived glioblastoma cell lines, demonstrating consistent inhibition on cell viability in vitro (Figure 2F and G, respectively). SKF96365 has already been shown to reduce calcium influx in glioma by acting on transient receptor potential canonical (TRPC) channels.[22,24–26] We confirmed that DPI-201-106 has on-target effects[27] in glioblastoma cells by modulating voltage-gated sodium channel currents and reducing the peak inward sodium current in GBM39 cells (Supplementary Figure 1).

SKF96365 and DPI-201-106 Reduce Glioblastoma Viability In Vitro by Altering the Cell Cycle

We next considered the impact of SKF96365 and DPI-201-106 treatment on affecting glioblastoma cell cycle progression. Across all 3 glioblastoma cell lines, SKF96365 was found to significantly induce cell cycle arrest in the G2/M phase of the cell cycle (Figure 3A-C, $P < .0001$). Treatment with DPI-201-106, however, caused variable cell cycle alterations across the glioblastoma cell lines (Figure 3D-F). Notably, GBM6 cells treated with DPI-201-106 had a significant increase in cells arrested in the S phase (Figure 3D, $P < .0001$). We further analyzed the levels of apoptosis after 3 and 7 days of drug treatment, and interestingly, there was only a significant increase in apoptosis after 7 days of SKF96365 treatment in all glioblastoma cell lines (Figure 3G-I). DPI-201-106 treatment significantly increased apoptosis levels after 7 days in GBM6 and GBM39 cells, but not SB2 cells (Figure 3G-I). This suggests that SKF96365 and DPI-201-106 impact cell cycle progression prior to cellular apoptosis.

To validate the indicative effects of SKF96365 and DPI-201-106 on modulating the cell cycle in glioblastoma cells in vitro, we examined the protein expression of cell cycle regulators p27 and p21 after treatment with either SKF96365 or DPI-201-106 for 24, 48, or 72 h. Overall, GBM6 cells displayed relatively weaker expression of p21 compared with GBM39 and SB2 cells (Figure 3J-L), likely owing to the TP53 (R273C) mutation present in GBM6 cells.[28] Compared with vehicle-treated cells, p21 levels were elevated by 24 h after treatment with DPI-201-106 in GBM6 (Figure 3J, with quantifications shown in Supplementary Figure 2A) and GBM39 (Figure 3K and Supplementary Figure 2B) but were increased in SB2 after treatment with SKF96365 by 48 h (Figure 3L and Supplementary Figure 2C). In contrast, p27 levels were mostly unaffected by DPI-201-106 treatment across the cell lines (Figure 3J-L and Supplementary Figure 2D-F). However, SKF96365

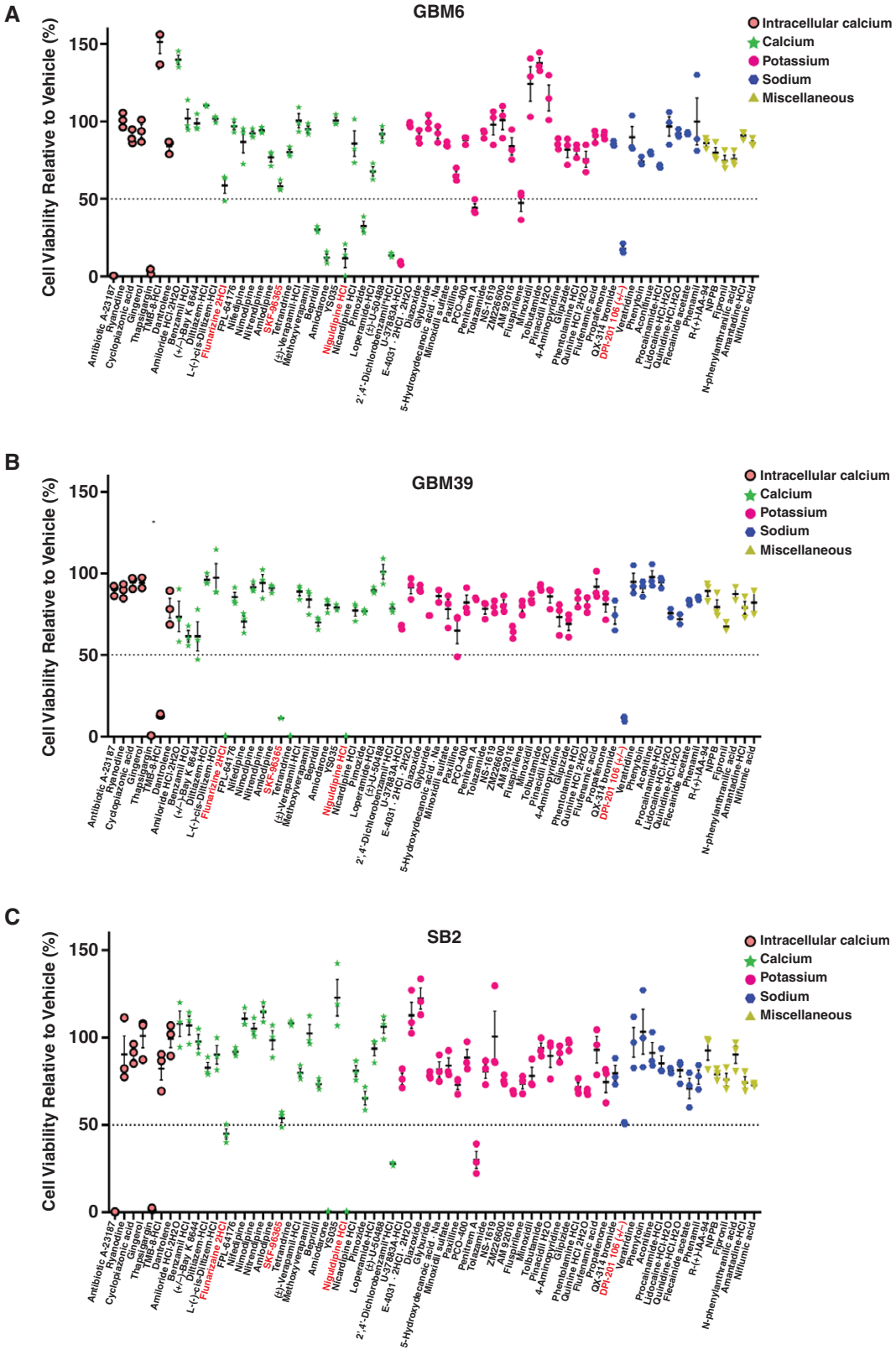

Figure 1. Drug screen identified ion channel modulators as inhibitors of glioblastoma growth. Cell viability after 7 days of treatment with the indicated drugs (10 μM) from an ion channel drug library in (A) GBM6, (B) GBM39, and (C) SB2. Data shown are mean ± SD. The horizontal dotted line shows 50% cell viability relative to vehicle-treated controls.

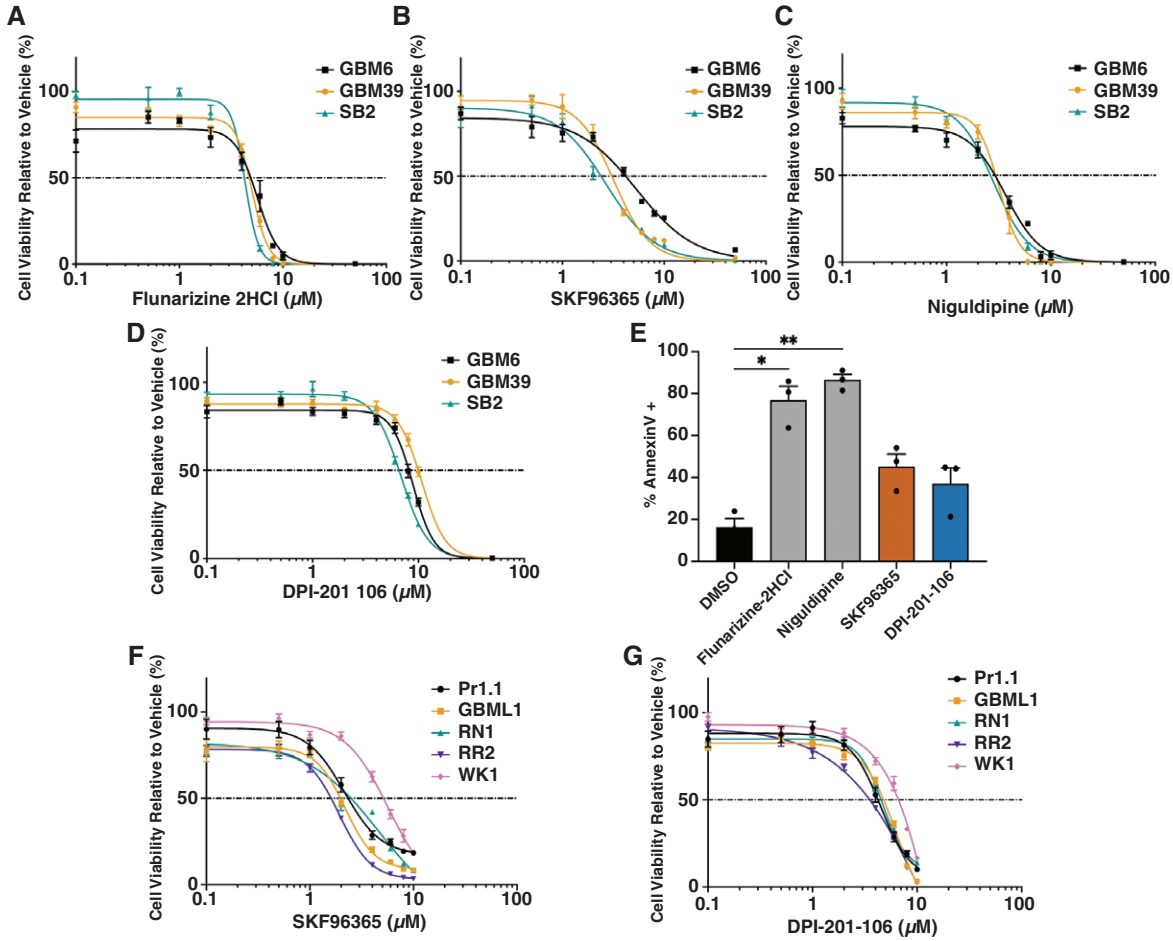

Figure 2. Dose-response validation of selected ion channel modulators in patient-derived glioblastoma cell lines. Dose-response was validated for (A) flunarizine-2HCl, (B) SKF96365, (C) niguldipine, and (D) DPI-201-106 in 3 patient-derived glioblastoma cell lines. (E) GBM6 cells were treated with DMSO, flunarizine-2HCl, niguldipine, SKF96365, or DPI-201-106 for 7 days to analyze levels of apoptosis by flow cytometry. Data shown are mean ± SD, and statistical significance was determined with a 1-way ANOVA and Dunnett's multiple comparison test. Dose-response curves of (F) SKF96365 and (G) DPI-201-106 were validated in 5 additional patient-derived primary glioblastoma cell lines. $^{*}P < .05$, $^{**}P < .01$.

demonstrated a trend toward increased p27 expression in GBM6 (Figure 3J and Supplementary Figure 2D) and GBM39 (Figure 3K and Supplementary Figure 2E), although nonsignificantly, whereas SKF96365 significantly decreased p27 expression in SB2 after 48 h (Figure 3L and Supplementary Figure 2F). Thus, the mechanisms underlying cell cycle blockade appear driven largely by increased levels of p21.

Since our cell cycle analysis showed SKF96365-treated glioblastoma cell lines were arrested in G2/M, we next considered if this effect was caused by mitotic arrest. In vehicle-treated cells, levels of cyclin B1 peaked at 10 h in all glioblastoma cell lines followed by degradation, demonstrating progression through mitosis. Glioblastoma cells treated with SKF96365 showed a slight delay in the degradation of cyclin B with elevated levels after 24 h (Figure 3 M-O). Similarly, phosphorylated CDK1 (p-CDK1) levels remain elevated after 10 h relative to control cells, demonstrating that SKF96365 delays mitosis but does not block it completely (Figure 3 M-O).

Efficacy of Ion Channel Drugs in Combination With Prexasertib in Glioblastoma In Vitro

Although p21 inhibits CDKs,[29] our data indicate that some cells can overcome this G2/M arrest and continue cycling. Therefore, we reasoned that other cell cycle inhibitors may synergize with ion channel inhibition. Prexasertib is a brain-penetrant, selective small molecule inhibitor of CHK1.[30] Activation of CHK1 is a critical mediator of both S and G2/M cell cycle arrest in the DNA damage response (DDR) pathway, leading to the inhibition of CDK activation and cell cycle progression, with particularly important roles in the maintenance of G2 arrest in p53-mutant cells. In the presence of DNA damage, blockade of CHK1 kinase activity with prexasertib forces cells to progress through mitosis, leading to the accumulation of DNA damage and apoptosis. We examined the effects of prexasertib on glioblastoma cells and found prexasertib to be effective at inhibiting cell viability in vitro (Figure 4A). Thus, we hypothesized that prexasertib would synergize with

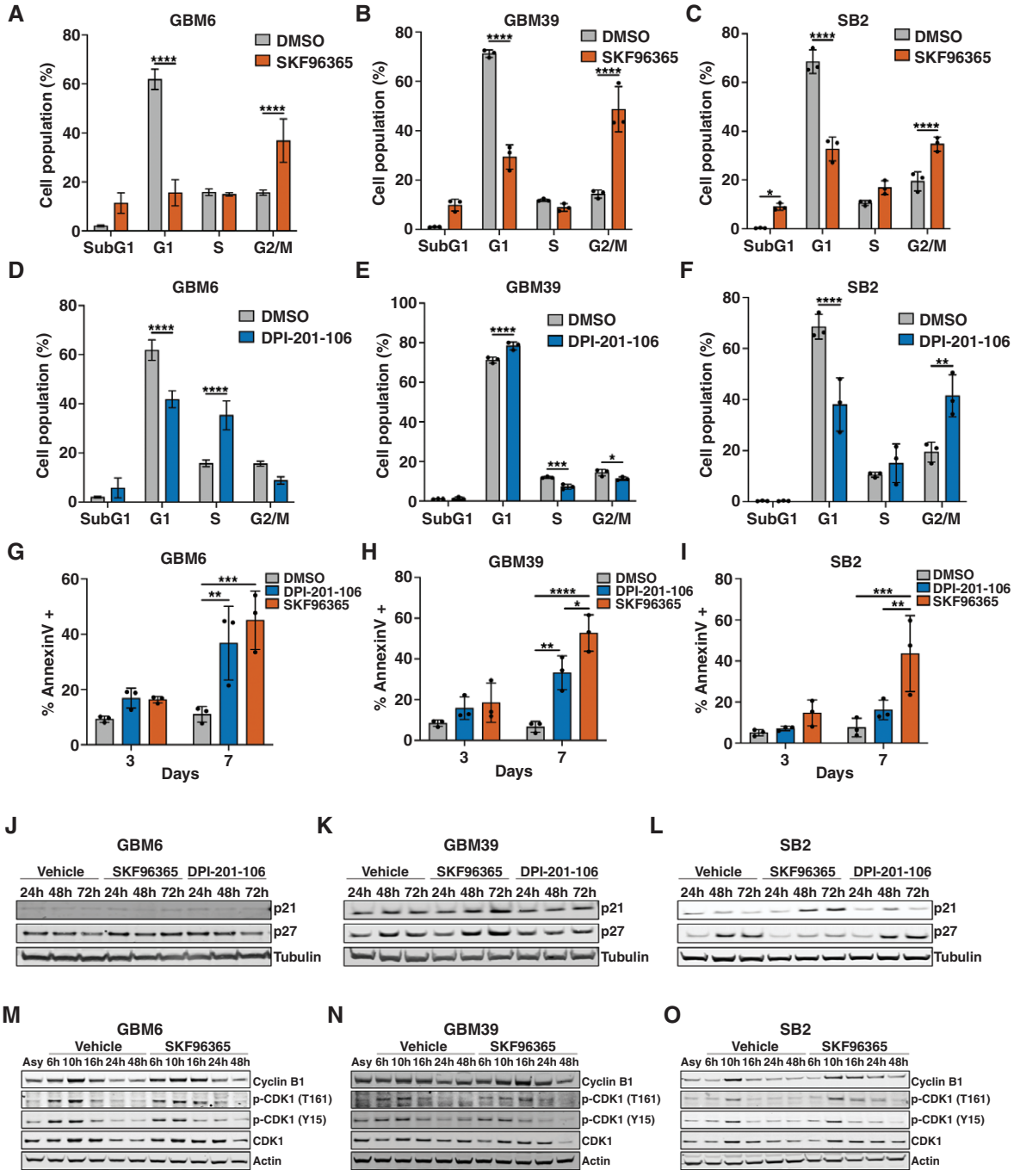

Figure 3. SKF96365 and DPI-201-106 induce cell cycle arrest in glioblastoma patient-derived cell lines. GBM6, GBM39, and SB2 cells were treated with 10 μM of SKF96365 (A-C) or DPI-201-106 (D-F), and the cell cycle was analyzed after 3 days. Data shown are mean ± SD and statistical significance was determined with a 2-way ANOVA and Šidák's multiple comparison test. Apoptosis was determined after treatment with 10 μM SKF96365 or DPI-201-106 after 3 and 7 days in (G) GBM, (H) GBM39, or (I) SB2. Data shown are mean ± SD, and statistical significance was determined with a 2-ANOVA and Dunnett's multiple comparison test. p21 and p27 expression was determined after 24, 48, and 72 h after treatment with 10 μM SKF96365 or DPI-201-106 in (J) GBM6, (K) GBM39, or (L) SB2 cells. The cell cycle was synchronized with a double thymidine block in SKF96365 or DPI-201-106-treated (M) GBM6, (N) GBM39, and (O) SB2 cells to analyze mitotic markers. Asynchronized cells (Asy) are shown as controls. *$P < .05$, **$P < .01$, ***$P < .001$, ****$P < .0001$.

SKF96365 and DPI-201-106 by preventing CHK1-mediated CDK1 inhibition, enhancing the cytotoxic effects of the ion channel modulators.

To determine the effects of combining ion channel inhibitors SKF96365 and DPI-201-106 with prexasertib, a dose-response matrix was performed with prexasertib alone or

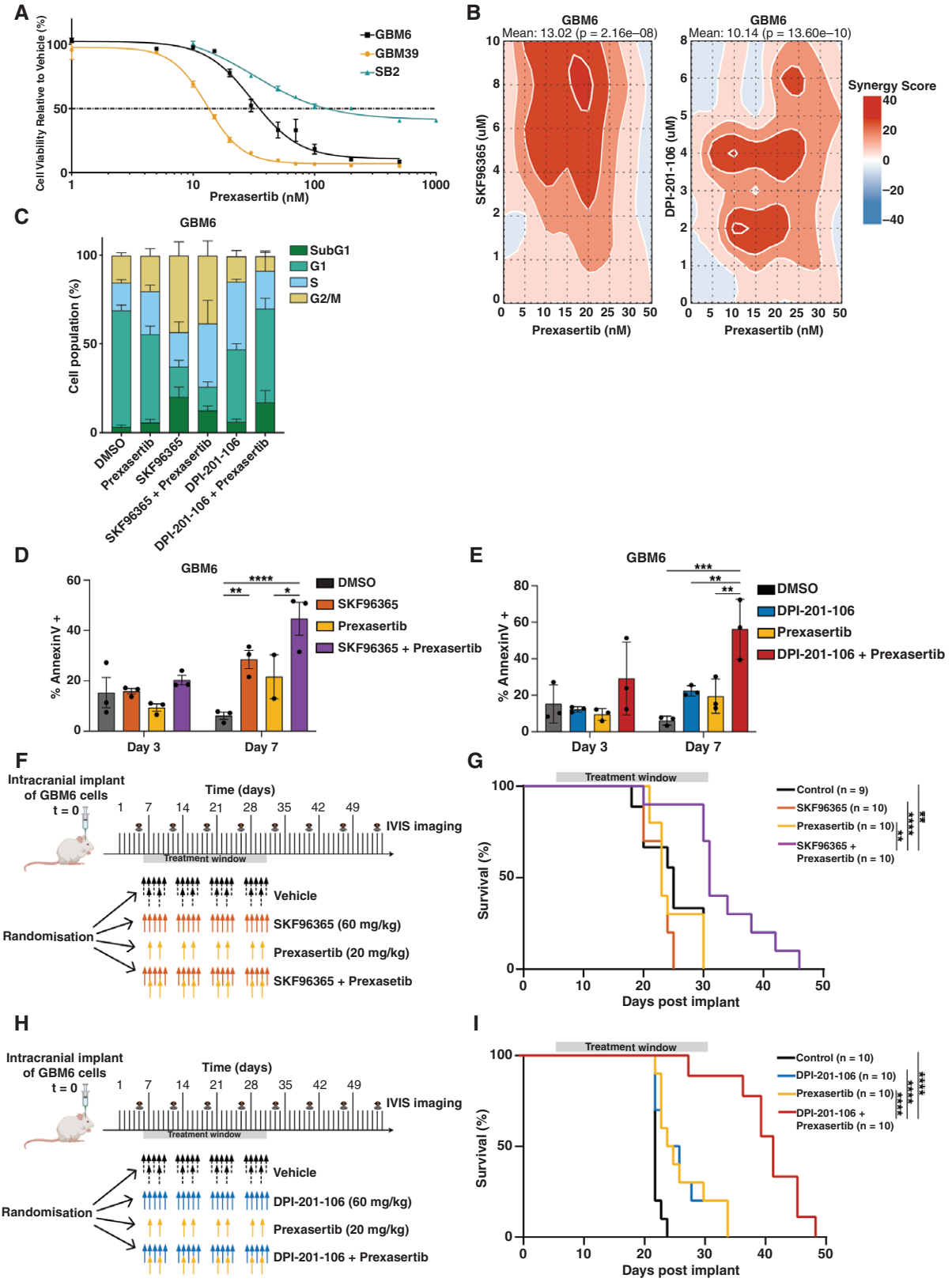

Figure 4. Combination treatment of ion channel drugs with prexasertib inhibits glioblastoma growth. (A) Dose-response of prexasertib on GBM6, GBM39, and SB2 cells after 7 days of treatment, where the horizontal dotted line shows 50% cell viability relative to DMSO controls. Data shown are mean ± SEM. (B) ZIP synergy scores were determined for GBM6 cells treated for 7 days with a dose combination matrix of prexasertib plus DPI-201-106 or SKF96365, as determined using SynergyFinder. (C) Cell cycle analysis was performed in GBM6 cells treated with 10 μM of either

SKF96365 or DPI-201-106 as a single agent or in combination with 30 nM of prexasertib after 3 days. Data shown are mean ± SD. AnnexinV apoptosis analysis was examined in GBM6 cells treated with 10 μM of either (D) SKF96365 or (E) DPI-201-106 as a single agent or in combination with 30 nM of prexasertib after 3 and 7 days. Data shown are mean ± SD, and statistical significance was determined with 2-way ANOVA and Tukey's multiple comparison test. (E) Schematic representation of the treatment protocol for the GBM6 orthograft mouse model where Balb/c nude mice with GBM6 tumors were treated as indicated in (F) and (H). (G) Kaplan-Meier survival curve of GBM6-bearing mice treated with vehicle, SKF96365, prexasertib, or a combination of SKF96365 and prexasertib. (I) Kaplan-Meier survival curve of GBM6-bearing mice treated with vehicle, DPI-201-106, prexasertib, or a combination of DPI-201-106 and prexasertib. Statistical significance was determined between the combination treatment and the other treatment groups with a log-rank (Mantel-Cox) test. *$P < .05$, **$P < .01$, ***$P < .001$, ****$P < .0001$, $P \geqq .01667$.

in combination with either SKF96365 or DPI-201-106. Drug interactions were analyzed using the SynergyFinder R package using the zero interaction potency (ZIP) model,[31] where a value of zero indicates the 2 drugs do not potentiate each other, whereas positive values indicate synergy. In agreement with our hypothesis, the combination of prexasertib plus SKF96365 and prexasertib plus DPI-201-106 had potently synergistic effects on reducing GBM6 cell viability, where the SKF96365 combination had a mean ZIP Synergy score of 13.02 ($P < .0001$, Figure 4B) and the DPI-201-106 combination had a mean ZIP Synergy score of 10.14 ($P < .0001$, Figure 4B). Interestingly, GBM39 only demonstrated statistically significant synergy in the DPI-201-106 combination (mean ZIP Synergy score of 6.71, $P < .01$, Supplementary Figure 3A). SB2 cells did not show a synergistic response from either combination treatment (Supplementary Figure 3B). To confirm the drug-drug interaction analysis, synergy was also assessed using an additional 3 drug interaction models: Loewe additivity (Loewe),[32] highest single agent,[33] and Bliss independence (Bliss).[34] Both prexasertib drug combinations resulted in consistent scores demonstrating overall synergy across the other 3 synergy models in GBM6 (Supplementary Figure 3C). The same patterns that were observed for the ZIP synergy scores in GBM39 and SB2 combination treatments were also observed across the other 3 synergy models (Supplementary Figure 3D and E).

We examined how the addition of prexasertib affects the cell cycle in TP53-mutant GBM6 cells, as they were the most responsive to the combination treatment. As expected, treatment with prexasertib alone significantly reduced the percentage of cells in G1 ($P < .05$) and slightly increased the percentage of cells in S phase, demonstrating the promotion of DNA synthesis and forced progression through the cell cycle, and nonsignificantly increased levels of apoptosis after 7 days (Figure 4C-E). The combination of prexasertib plus SKF96365 treatment showed similar cell cycle ratios to that observed in GBM6 cells treated with SKF96365 alone (Figure 4C). In addition, the combination treatment of prexasertib plus SKF96365 had significantly increased levels of apoptotic cells at day 7 compared with control cells and prexasertib alone but was not significantly increased compared with the single SKF96365 treatment (Figure 4D). On the other hand, the combination of DPI-201-106 plus prexasertib significantly reduced the S phase arrest observed in single DPI-201-106 treatment ($P < .01$) and nonsignificantly increased the number of cells in subG1 (Figure 4C). Furthermore, the combination treatment significantly increased the percentage of apoptotic cells after 7 days compared with both prexasertib and DPI-201-106 alone (Figure 4E).

Combining Ion Channel Drugs With Prexasertib Significantly Improves Survival in Orthotopic Mouse Models

Given the in vitro synergy observed when prexasertib was combined with ion channel inhibitors, we evaluated the combination of SKF96365 or DPI-201-106 with prexasertib in a GBM6 orthotopic xenograft model. Transgenic GBM6 cells expressing luciferase and GFP were implanted in the frontal cortex of 6 to 7-week-old Balb/c nude female mice ($t = 0$). On day 5, tumor growth was monitored by bioluminescence and mice were randomized into 4 groups prior to treatment on day 6 according to the experimental design shown in Figure 4F and H.

GBM6-bearing mice treated with the SKF96365 plus prexasertib showed a significant extension of survival compared with vehicle control and the single-agent treatments (Figure 4G). The median survival for vehicle-treated mice, SKF96365-treated mice, and prexasertib-treated mice was similar across the groups, at 25, 23, and 23 days, respectively, whereas the combination-treated mice had a significantly extended median survival of 31 days. Similarly, there was no difference in survival in GBM6-bearing mice treated with either DPI-201-106 alone (Figure 4I). Relative to SKF96365 treatment, combining DPI-201-106 with prexasertib was even more effective, significantly extending median survival to 42 days compared with control-treated mice (22 days, $P < .001$, Figure 4I). No significant weight loss was observed in any of the groups (Supplementary Figure 4A and B).

DPI-201-106 as a Novel Therapeutic Agent for Glioblastoma in Combination With Prexasertib

The results shown thus far demonstrate that DPI-201-106 is a promising therapeutic agent that shows enhanced and synergistic efficacy when combined with prexasertib. To reinforce our novel strategy, we next validated the effects of DPI-201-106 in a second glioblastoma model. WK1 is a primary classical patient-derived glioblastoma cell line that produces a slower growing xenograft model relative to GBM6. Firstly, we examined the effects of prexasertib and DPI-201-106 on WK1 cells in vitro. WK1 cells treated with prexasertib demonstrated a similar dose-response to the other cell lines (Supplementary Figure 5A). In contrast to GBM6, the combination of DPI-201-106 with prexasertib had a significant antagonistic effect on WK1 cells ($P < .0001$; Supplementary Figure 5B and C). Furthermore, cell cycle analysis showed no substantial changes in WK1 cells treated with DPI-201-106 alone nor in combination with prexasertib (Supplementary

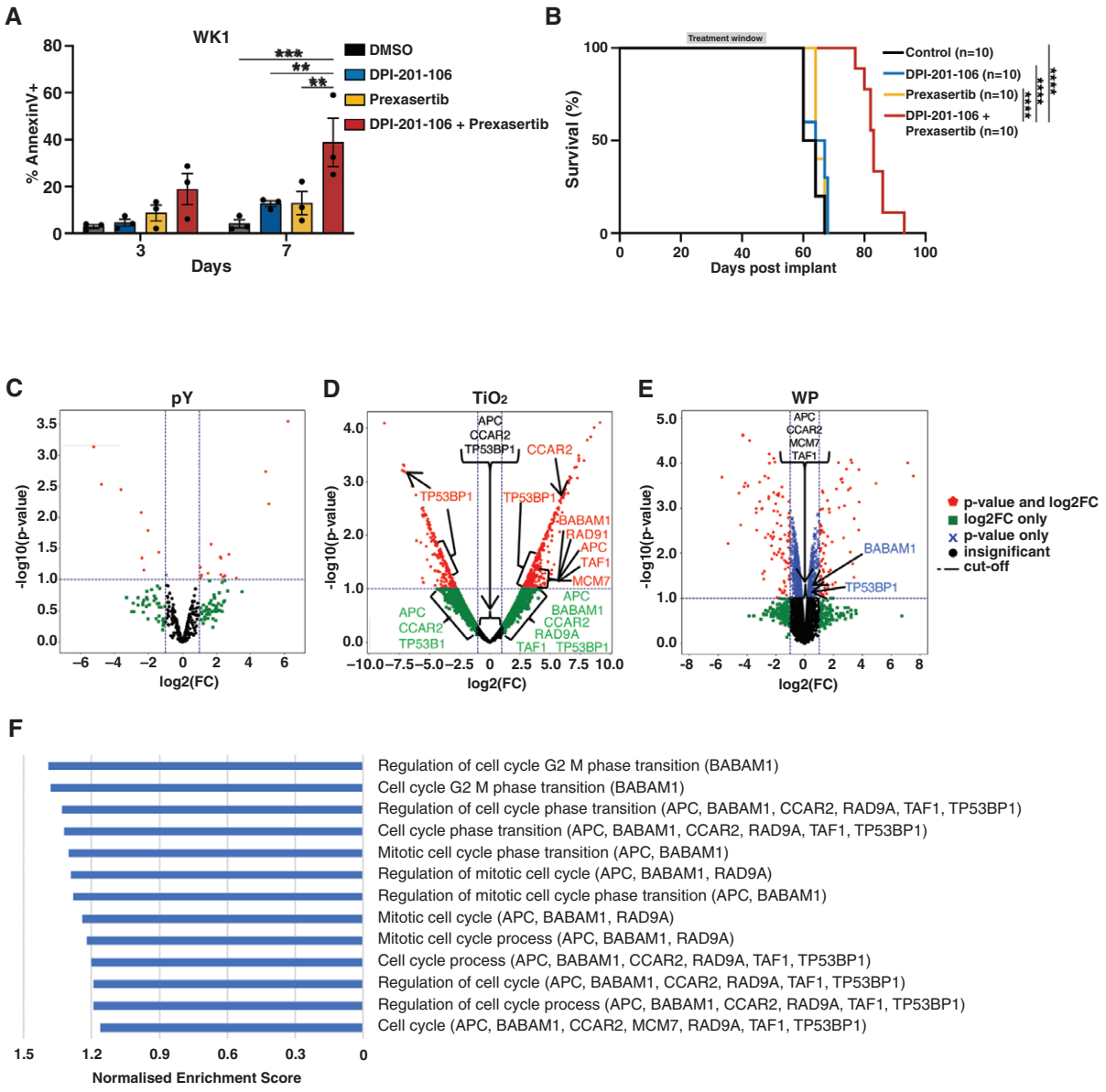

Figure 5. DPI-201-106 validation in a WK1 glioblastoma model. (A) AnnexinV apoptosis analysis was examined in WK1 cells treated with 10 μM DPI-201-106 after 3 and 7 days. Data shown are mean ± SD, and statistical significance was determined with a 2-ANOVA and Tukey's multiple comparison test. (B) Kaplan-Meier survival curve of WK1-bearing mice treated with vehicle, DPI-201-106, prexasertib, or a combination of DPI-201-106 and prexasertib. Data are presented as the percentage survival of mice in each group where statistical significance was determined between the combination treatment and the other treatment groups with a log-rank (Mantel-Cox) test. Mass spectrometry analysis was performed on WK1 cells treated with DPI-201-106 for 24 h and volcano plots for (C) tyrosine phosphorylated peptides, (D) serine/threonine phosphorylated peptides, and (E) whole protein peptides were generated using Python. (F) Normalized enrichment scores of significant gene sets identified by GSEA of serine/threonine phosphorylated peptides in DPI-201-106-treated WK1 cells. $^{**}p < .01$, $^{***}P < .001$, $^{****}P < .0001$. pY, tyrosine phosphorylated; TiO_2, serine/threonine phosphorylated; WP, whole protein.

Figure 5D). However, WK1 cells treated with the combination of DPI-201-106 plus prexasertib still had significantly increased levels of apoptosis after 7 days compared with either treatment alone (Figure 5A). Therefore, we tested the DPI-201-106 plus prexasertib combination in vivo in a WK1 xenograft model. As a slower growing model, WK1-bearing mice monitored for tumor growth prior to randomization on day 22, followed by the same treatment schedule used in the GBM6 model starting on day 23. Despite our in vitro data suggesting that this drug combination has an antagonistic effect on WK1 cell viability, WK1-bearing mice had significantly improved survival following combination treatment compared with vehicle-treated animals (median survival 83 versus 62 days, respectively, $P < .0001$), with DPI-201-106 or prexasertib monotherapy having no effect (median survival 65.6 and 64 days, respectively) (Figure 5B).

Table 1. Enriched Gene Sets of Interest Identified by DAVID in DPI_TiO2_WK1

Source	Identifier	Gene set	*P*-value
GOBP	GO:0006974	Cellular response to DNA damage stimulus	.0029
GOBP	GO:0045739	Positive regulation of DNA repair	.0177
GOBP	GO:0007049	Cell cycle	.0124
Reactome	R-HSA-1640170	Cell cycle	.0127
GOBP	GO:2000134	Negative regulation of G1/S transition of mitotic cell cycle	.0325

Abbreviation: GOBP, Gene Ontology Biological Processes.

We originally proposed that the combination of DPI-201-106 and prexasertib was functioning through modulation of the cell cycle; however, our WK1 in vitro data suggest that that is not necessarily the case; yet we still demonstrated a striking synergistic effect in vivo. Notably, as CHK1 inhibition prevents cell cycle arrest, it, therefore, impedes DNA damage repair not only indirectly by blocking activation of the cell cycle checkpoints that provide time for DNA repair to occur, but also directly by activating downstream DNA repair factors, including Rad51[35] and FANCE,[36] mediators of the homologous recombination repair pathway and Fanconi anemia/BRCA repair pathway, respectively. Collectively, our WK1 model indicates that DPI-201-106 and prexasertib may also synergize around DNA damage mechanisms. To investigate this, we performed mass spectrometry analysis on WK1 cells treated with DPI-201-106 to identify drug-induced changes in WP abundance and possible changes in protein phosphorylation (tyrosine phosphorylated, pY; serine/threonine phosphorylated, TiO_2). Differentially expressed proteins were identified using statistical thresholds best visualized by volcano plots. Identified phosphopeptides with altered abundance and their associated information are listed in Supplementary Tables 4-6. From the pY data analysis, 15 (4.1%) and 8 (2.2%) of phosphopeptides exhibited increased and decreased abundance, respectively (Figure 5C). The TiO_2-enriched data analysis identified 342 (3.8%) and 211 (2.3%) phosphopeptides with increased and decreased abundance, respectively (Figure 5D). In terms of protein expression, 79 (1.4%) and 90 (1.6%) peptides displayed identified increased and decreased abundance, respectively (Figure 5E). DAVID was used to identify differentially represented pathways associated with DPI-201-106 treatment in WK1 cells. Identified up- and downregulated pathways are listed in Supplementary Tables 7-9. Two gene sets related to DNA damage and 3 cell cycle gene sets were significantly upregulated in TiO2-enriched phosphopeptides from DPI-201-106-treated WK1 cells (Table 1). Within these gene sets 3 proteins, TP53BP1, MCM7, and RAD9A, were common among the DNA damage (GO:0006974) and cell cycle regulation (R-HAS-1640170) pathways (Supplementary Table 10). To further explore how DPI-201-106 affects DNA damage and the cell cycle in WK1 cells, GSEA was performed on the genes associated with the identified phosphosites with altered abundance using DNA damage and cell cycle gene sets obtained from MSigDB. None of the differentially expressed proteins/phosphosites identified had enrichment in DNA damage gene sets that reached statistical significance (Supplementary Tables 11-13). While there were no cell cycle gene sets that achieved significance for tyrosine phosphorylated peptides or whole proteins (Supplementary Tables 14 and 16), there were 13 significantly upregulated gene sets for serine/threonine phosphorylated peptides (Figure 5F and Supplementary Table 15). All other gene sets identified from the differentially expressed peptides are described in Supplementary Tables 17-19.

DPI-201-106 Works in Synergy With Other DDR Inhibitors to Reduce Glioblastoma Growth

Since DPI-201-106 proved to have the greatest synergistic effects with prexasertib in glioblastoma both in vitro and in vivo, and demonstrated involvement in DNA damage repair, we considered whether DPI-201-106 could be combined with other inhibitors known to block the DDR pathway. As a proof of principle, a dose-response matrix was performed in GBM6 cells in vitro with DPI-201-106 alone or in combination with other inhibitors of the DDR pathway, including niraparib (PARP inhibitor), SOL578 (CHK1 inhibitor), ceralasertib (ATR inhibitor), and adavosertib (Wee1 inhibitor) and the data were analyzed using the SynergyFinder R package. The combination of DPI-201-106 plus niraparib was synergistic in GBM6 cells (mean ZIP score 8.38, $P < .001$, Supplementary Figure 6A). DPI-201-106 in combination with SOL578, a second CHK1 inhibitor, displayed both synergistic and antagonistic effects depending on the dose of SOL578 (mean ZIP score 2.29, $P < .02$, Supplementary Figure 6B). Both the ceralasertib and the adavosertib combination with DPI-201-106 demonstrated antagonistic effects in GBM6 cells (Supplementary Figure 6C and D). Therefore, we next validated the DPI-201-106 plus niraparib combination in our GBM6 orthotopic model (Supplementary Figure 7A). Like the DPI-201-106 plus prexasertib combination, the combination treatment of DPI-201-106 plus niraparib resulted in significantly improved survival of GBM6-bearing mice compared with control mice and mice treated with either DPI-201-106 or niraparib alone (median survival 47, 30, 32, and 36 days, respectively; $P < .0001$, Supplementary Figure 7B). This validates that the combination of DPI-201-106 with DDR inhibitors is a novel and unique therapeutic strategy for glioblastoma.

Discussion

In this discovery study, we performed an ion channel drug screen on patient-derived glioblastoma cells. SKF96365 and DPI-201-106 had antiproliferative activity, inhibited the cell cycle in vitro, and demonstrated synergistic effects when combined with a CHK1 inhibitor, prexasertib. SKF96365 has inhibitory activity on TRPC channels, thereby reducing calcium influx.[22,24-26] Our results agree with previous studies that have demonstrated that SKF96365 induces cell cycle arrest in the G2 phase in glioma cells.[22,24] This is unsurprising as intracellular calcium is required for cell cycle progression and mitosis entry. For the first time, this study identified DPI-201-106 as a compound displaying novel anticancer activity in glioblastoma. As a sodium channel modifier, DPI-201-106 was initially evaluated as a treatment for congestive heart failure.[37,38] We now show that DPI-201-106 treatment may impact the DDR pathways in glioblastoma, and consequently, impeding the cell cycle. DPI-201-106 was synergistic with DDR inhibitors, improving the survival of orthotopic glioblastoma xenografts in mice. The combination of DPI-201-106 and prexasertib showed superior effects to that of SKF96365 and prexasertib in vivo, extending the median survival by 20 days in 2 different patient-derived xenograft models. In support of this observation, we also showed that DPI-201-106 also synergized with the PARP inhibitor niraparib, a different class of DDR inhibitors.

Activation of DDR pathways in glioblastoma plays a significant role in pathogenesis and treatment resistance.[39] Indeed, in the SOC treatment for glioblastoma, both TMZ and RT induce DNA damage in brain cancer cells. Given this, our results indicate that DPI-201-106 may be a promising agent to combine with RT. Targeting DNA damage in brain cancer is a rational approach, but drugs that inhibit DDR have not been extensively evaluated, largely due to their limited BBB penetrance.[40] Prexasertib is in clinical development and has been evaluated in phase II clinical trials for other solid tumors.[40-43] Therefore, the pharmacokinetics and safety have been fully evaluated in humans, and preclinical medulloblastoma models have shown that it can cross the BBB,[30] but its efficacy in human brain tumors remains to be elucidated.[40,44] The PARP inhibitor niraparib is FDA approved for ovarian cancer[45] and has demonstrated superior BBB penetrance in preclinical models compared with other PARP inhibitors.[46,47] Furthermore, a case report demonstrated clinical activity in a patient with brain metastases.[48] Although DPI-201-106 is not yet approved by FDA, the safety and tolerability of dosing have already been established in healthy people[49] and have been used off-label for treating cardiac failure.[37] To validate the potential toxicity on neuronal cells, we have tested our working concentration of DPI-201-106 in a 3D model of human brain tissue in vitro and demonstrated no change in cytotoxicity or loss of cell viability (data not shown). Thus, the significance of our drug combination discovery lies in the rapid translatability of combining DPI-201-106 and niraparib/prexasertib into clinical trials for brain cancer patients. We have preliminary data demonstrating that DPI-201-106 plus niraparib is also effective in vitro against pediatric diffuse midline glioma, as well as showing efficacy as a single agent in medulloblastoma and ependymoma cells, indicating that DPI-201-106 may be a suitable treatment to explore across a range of brain tumors for adults and children.

Recent work has shown that activation of sodium channels using another sodium channel modulator, cypermethrin, results in reduced cell viability, cell cycle arrest, and increased protein expression of DNA repair–related markers in neuroblastoma cells.[50] This result is similar to our findings that indicated DPI-201-106 exerts its anticancer effects by modulating the cell cycle and DDR pathways; however, the exact mechanism of this is unknown. It may be speculated that a DPI-201-106-induced net influx of Na^+ causes an intracellular Ca^{2+} overload in glioblastoma cells, as this effect has been shown to occur in cardiac muscle.[51] Cellular calcium and sodium homeostasis has been shown to be critical for mitochondrial function in neurons,[52] and mitochondrial dysfunction has been shown to negatively impact nuclear DDR signaling pathways.[53] Therefore, there may be an intricate link between ionic flux, mitochondrial function, and DDR pathways in brain cancer, but this remains to be elucidated. Furthermore, it is unclear how our novel combination compares to the current SOC treatments, which is beyond the scope of this work.

In summary, we discovered that the ion channel modulator DPI-201-106 is a novel drug for enhancing the cell-killing properties of DDR inhibitors in brain cancer. Through modulation of the cell cycle and DDR mechanisms, DPI-201-106 is a promising agent to explore in future clinical studies, either incorporating with current SOC treatments or as a novel synergistic combination approach with DDR inhibitors, such as prexasertib or niraparib.

Supplementary material

Supplementary material is available online at *Neuro-Oncology Advances* (https://academic.oup.com/noa).

Keywords

cell cycle | DNA damage | glioblastoma | ion channel.

Lay Summary

Glioblastoma is an aggressive type of brain cancer. Proteins in cells called ion channels help relay signals between cells and may play a role in cancer growth. The authors of this study wanted to see if blocking ion channels could help treat glioblastoma. To do this, they tested 72 drugs on glioblastoma cells taken from patient tumors. Their results showed that 1 drug, called DPI-201-106, stopped cancer cells from dividing and caused cell death. When they combined this drug with others that caused DNA damage, it worked even better, both in laboratory dishes and in mice with glioblastoma.

Funding

This work was supported by the Pirate Ship Foundation, The Cure Starts Now, Perth Children's Hospital Foundation, the Western Australian Future Health Research and Innovation Fund, The Brain Tumour Charity, and the Robert Connor Dawes Foundation. B.D. is supported by the BrightSpark Foundation and the Western Australian Future Health Research and Innovation Fund [ECR 003-2023]. R.E. is supported by a Cancer Council WA Research Fellowship and a Pirate Ship Foundation Brainchild Fellowship.

Acknowledgments

We are grateful to all patients and their families affected by brain cancer for their invaluable tissue donations and consumers who have provided input to our research. We thank all members of the Telethon Kids Institute Oncogenic Signalling Laboratory and Brain Tumour Research team for their advice, suggestions, and discussions. We acknowledge the significant contribution made by all the animals used in this study and thank the Bioresources team of Telethon Kids Institute for their care. We thank and acknowledge Sentinel Oncology Limited for providing SOL578 to conduct this work. We would like to acknowledge Monash Proteomics and Metabolomics Platform (MPMP) for expertise in sample preparation and mass spectrometry method development. Computational resources were supported by the R@CMon/Monash Node of the NeCTAR Research Cloud, an initiative of the Australian Government's Super Science Scheme and the Education Investment Fund.

Conflict of interest statement

T.G.J., J.P.F., M.K., and E.V.F. are named inventors on an international patent for the invention of the use of an ion channel inhibitor that inhibits the cell cycle and an inhibitor of CHK1, ATM, Wee1, ATR, or PARP in the treatment or prevention of cancer (PCT/AU2023/050462).

Authorship statement

All authors read and approved this manuscript. Conceptualization: B.D., T.G.J., P.J.M.; in vitro data collection: B.D., P.J.M., C.R., L.U., Z.Y.N, C.J.M.; in vivo data collection: M.K., R.P.; data analysis and interpretation: B.D., P.J.M, E.V.F., C.J.M., M.K., R.P., T.C.C.L.K.S, R.J.D., R.E., T.G.J.; funding acquisition: S.V., R.E., and T.G.J.; writing—original draft: B.D.; writing—draft revisions and editing: B.D., E.V.F., R.J.D., R.E., and T.G.J.

Data availability

Any data not presented in this manuscript will be made publicly available upon reasonable request.

Affiliations

The Kids Research Institute, Perth, Western Australia, Australia (B.D., P.J.M., C.R., Z.Y.N., L.U., E.V.F., M.K., R.P., S.V., R.E., T.G.J.); Division of Paediatrics/Centre for Child Health Research, Medical School, University of Western Australia, Western Australia, Australia (B.D., P.J.M., E.V.F., S.V., R.E., T.G.J.); Perth Children's Hospital, Perth, Western Australia, Australia (S.V.); Cancer Program, Biomedicine Discovery Institute and Department of Biochemistry and Molecular Biology, Monash University, Clayton, Victoria, Australia (R.J.D.); Florey Institute of Neuroscience and Mental Health, The University of Melbourne, Melbourne, Victoria, Australia (S.P., C.J.M.); Department of Medicine, The University of Melbourne, Melbourne, Victoria, Australia (S.P.); Monash Proteomics and Metabolomics Platform, Department of Biochemistry and Molecular Biology, Monash Biomedicine Discovery Institute, Monash University, Clayton, Victoria, Australia (T.C.C.L.K.S.)

References

1. Dewdney B, Jenkins MR, Best SA, et al. From signalling pathways to targeted therapies: unravelling glioblastoma's secrets and harnessing two decades of progress. *Signal Transduct Target Ther.* 2023;8(1):400.
2. Rapp M, Baernreuther J, Turowski B, et al. Recurrence pattern analysis of primary glioblastoma. *World Neurosurg.* 2017;103:733–740.
3. Simoens S, Huys I. R&D costs of new medicines: a landscape analysis. *Front Med (Lausanne).* 2021;8:760762.
4. Demirci E, Omes-Smit G, Zwiers A. Clinical development time is shorter for new anticancer drugs approved via accelerated approval in the US or via conditional approval in the EU. *Clin Transl Sci.* 2023;16(7):1127–1133.
5. Venkatesh HS, Morishita W, Geraghty AC, et al. Electrical and synaptic integration of glioma into neural circuits. *Nature.* 2019;573(7775):539–545.
6. Kumar P, Kumar D, Jha SK, Jha NK, Ambasta RK. Chapter three—ion channels in neurological disorders. In: Donev R, ed. *Advances in Protein Chemistry and Structural Biology.* Vol 103. United Kingdom: Academic Press; 2016:97–136.
7. Griffin M, Khan R, Basu S, Smith S. Ion channels as therapeutic targets in high grade gliomas. *Cancers (Basel).* 2020;12(10):3068.
8. Imbrici P, Liantonio A, Camerino GM, et al. Therapeutic approaches to genetic ion Channelopathies and perspectives in drug discovery. *Front Pharmacol.* 2016;7:121.
9. Shi DD, Guo JA, Hoffman HI, et al. Therapeutic avenues for cancer neuroscience: translational frontiers and clinical opportunities. *Lancet Oncol.* 2022;23(2):e62–e74.
10. Sarkaria JN, Carlson BL, Schroeder MA, et al. Use of an Orthotopic xenograft model for assessing the effect of epidermal growth factor receptor amplification on glioblastoma radiation response. *Clin Cancer Res.* 2006;12(7):2264–2271.
11. Stringer BW, Day BW, D'Souza RCJ, et al. A reference collection of patient-derived cell line and xenograft models of proneural, classical and mesenchymal glioblastoma. *Sci Rep.* 2019;9(1):4902.
12. Greenall SA, Lim YC, Mitchell CB, et al. Cyclin-dependent kinase 7 is a therapeutic target in high-grade glioma. *Oncogenesis.* 2017;6(5):e336.

13. Endersby R, Whitehouse J, Hii H, et al. A pre-clinical assessment of the pan-ERBB inhibitor dacomitinib in pediatric and adult brain tumors. *Neoplasia.* 2018;20(5):432–442.
14. Ianevski A, Giri AK, Aittokallio T. SynergyFinder 3.0: an interactive analysis and consensus interpretation of multi-drug synergies across multiple samples. *Nucleic Acids Res.* 2022;50(W1):W739–W743.
15. Petty SJ, Milligan CJ, Todaro M, et al. The antiepileptic medications carbamazepine and phenytoin inhibit native sodium currents in murine osteoblasts. *Epilepsia.* 2016;57(9):1398–1405.
16. Endersby R, Whitehouse J, Pribnow A, et al. Small-molecule screen reveals synergy of cell cycle checkpoint kinase inhibitors with DNA-damaging chemotherapies in medulloblastoma. *Sci Transl Med.* 2021;13(577).
17. Nguyen EV, Pereira BA, Lawrence MG, et al. Proteomic profiling of human prostate cancer-associated fibroblasts (CAF) reveals LOXL2-dependent regulation of the tumor microenvironment. *Mol Cell Proteomics.* 2019;18(7):1410–1427.
18. Fleuren EDG, Vlenterie M, van der Graaf WTA, et al. Phosphoproteomic profiling reveals ALK and MET as novel actionable targets across synovial sarcoma subtypes. *Cancer Res.* 2017;77(16):4279–4292.
19. Ritchie ME, Phipson B, Wu D, et al. limma powers differential expression analyses for RNA-sequencing and microarray studies. *Nucleic Acids Res.* 2015;43(7):e47.
20. Liberzon A, Subramanian A, Pinchback R, et al. Molecular signatures database (MSigDB) 3.0. *Bioinformatics.* 2011;27(12):1739–1740.
21. Zheng S, Wang W, Aldahdooh J, et al. SynergyFinder plus: toward better interpretation and annotation of drug combination screening datasets. *Genom Proteom Bioinform.* 2022;20(3):587–596.
22. Song M, Chen D, Yu SP. The TRPC channel blocker SKF 96365 inhibits glioblastoma cell growth by enhancing reverse mode of the Na(+) / Ca(2+) exchanger and increasing intracellular Ca(2+). *Br J Pharmacol.* 2014;171(14):3432–3447.
23. Niklasson M, Maddalo G, Sramkova Z, et al. Membrane-depolarizing channel blockers induce selective glioma cell death by impairing nutrient transport and unfolded protein/amino acid responses. *Cancer Res.* 2017;77(7):1741–1752.
24. Bomben VC, Sontheimer HW. Inhibition of transient receptor potential canonical channels impairs cytokinesis in human malignant gliomas. *Cell Prolif.* 2008;41(1):98–121.
25. Chigurupati S, Venkataraman R, Barrera D, et al. Receptor channel TRPC6 is a key mediator of notch-driven glioblastoma growth and invasiveness. *Cancer Res.* 2010;70(1):418–427.
26. Ding X, He Z, Zhou K, et al. Essential role of TRPC6 channels in G2/M phase transition and development of human glioma. *J Natl Cancer Inst.* 2010;102(14):1052–1068.
27. Krafte DS, Davison K, Dugrenier N, et al. Pharmacological modulation of human cardiac Na+ channels. *Eur J Pharmacol.* 1994;266(3):245–254.
28. Pandita A, Aldape KD, Zadeh G, Guha A, James CD. Contrasting in vivo and in vitro fates of glioblastoma cell subpopulations with amplified EGFR. *Genes Chromosomes Cancer.* 2004;39(1):29–36.
29. Xiong Y, Hannon GJ, Zhang H, et al. p21 is a universal inhibitor of cyclin kinases. *Nature.* 1993;366(6456):701–704.
30. Campagne O, Davis A, Maharaj AR, et al. CNS penetration and pharmacodynamics of the CHK1 inhibitor prexasertib in a mouse Group 3 medulloblastoma model. *Eur J Pharm Sci.* 2020;142:105106.
31. Yadav B, Wennerberg K, Aittokallio T, Tang J. Searching for drug synergy in complex dose-response landscapes using an interaction potency model. *Comput Struct Biotechnol J.* 2015;13:504–513.
32. Loewe S. The problem of synergism and antagonism of combined drugs. *Arzneimittelforschung.* 1953;3(6):285–290.
33. Berenbaum MC. What is synergy? *Pharmacol Rev.* 1989;41(2):93–141.
34. Bliss CI. The toxicity of poisons applied jointly. *Ann Appl Biol.* 1939;26(3):585–615.
35. Sørensen CS, Hansen LT, Dziegielewski J, et al. The cell-cycle checkpoint kinase Chk1 is required for mammalian homologous recombination repair. *Nat Cell Biol.* 2005;7(2):195–201.
36. Wang X, Kennedy RD, Ray K, et al. Chk1-mediated phosphorylation of FANCE is required for the Fanconi anemia/BRCA pathway. *Mol Cell Biol.* 2007;27(8):3098–3108.
37. Kostis JB, Lacy CR, Raia JJ, et al. DPI 201-106 for severe congestive heart failure. *Am J Cardiol.* 1987;60(16):1334–1339.
38. Hogan JC, Greenbaum RA, Lunnon MW, Hilson AJ, Evans TR. Haemodynamic effects of DPI 201-106, following single intravenous dose administration to patients with moderate cardiac failure. *Eur Heart J.* 1988;9(5):498–502.
39. Bao S, Wu Q, McLendon RE, et al. Glioma stem cells promote radioresistance by preferential activation of the DNA damage response. *Nature.* 2006;444(7120):756–760.
40. Majd NK, Yap TA, Koul D, et al. The promise of DNA damage response inhibitors for the treatment of glioblastoma. *Neurooncol. Adv.* 2021;3(1).
41. Gupta N, Huang TT, Nair JR, et al. BLM overexpression as a predictive biomarker for CHK1 inhibitor response in PARP inhibitor-resistant BRCA-mutant ovarian cancer. *Sci Transl Med.* 2023;15(701):eadd7872.
42. Konstantinopoulos PA, Lee JM, Gao B, et al. A Phase 2 study of prexasertib (LY2606368) in platinum resistant or refractory recurrent ovarian cancer. *Gynecol Oncol.* 2022;167(2):213–225.
43. Slotkin EK, Mauguen A, Ortiz MV, et al. A phase I/II study of prexasertib in combination with irinotecan in patients with relapsed/refractory desmoplastic small round cell tumor and rhabdomyosarcoma. *J Clin Oncol.* 2022;40(16_suppl):11503–11503.
44. Cash T, Fox E, Liu X, et al. A phase 1 study of prexasertib (LY2606368), a CHK1/2 inhibitor, in pediatric patients with recurrent or refractory solid tumors, including CNS tumors: a report from the children's oncology group pediatric early phase clinical trials network (ADVL1515). *Pediatr Blood Cancer.* 2021;68(9):e29065.
45. Ison G, Howie LJ, Amiri-Kordestani L, et al. FDA approval summary: niraparib for the maintenance treatment of patients with recurrent ovarian cancer in response to platinum-based chemotherapy. *Clin Cancer Res.* 2018;24(17):4066–4071.
46. Gada K, Sharma G, Kmett C, et al. Tissue distribution and brain penetration of niraparib in tumor bearing mouse models and its clinical relevance. *J Clin Oncol.* 2021;39(15_suppl):e15066–e15066.
47. Sun K, Mikule K, Wang Z, et al. A comparative pharmacokinetic study of PARP inhibitors demonstrates favorable properties for niraparib efficacy in preclinical tumor models. *Oncotarget.* 2018;9(98):37080–37096.
48. Wang Q, Zhang F, Gao H, Xu Y. Successful treatment of a patient with brain metastases from endometrial cancer using niraparib: a case report. *Ann Palliat Med.* 2021;10(1):818–827.
49. Rüegg PC, Nüesch E. The effect of a new inotropic agent, DPI 201-106, on systolic time intervals and the electrocardiogram in healthy subjects. *Br J Clin Pharmacol.* 1987;24(4):453–458.
50. Promthep K, Nopparat C, Mukda S, et al. Proteomic profiling reveals neuronal ion channel dysregulation and cellular responses to DNA damage-induced cell cycle arrest and senescence in human neuroblastoma SH-SY5Y cells exposed to cypermethrin. *Neurotoxicology.* 2022;93:71–83.
51. Gwathmey JK, Slawsky MT, Briggs GM, Morgan JP. Role of intracellular sodium in the regulation of intracellular calcium and contractility. Effects of DPI 201-106 on excitation-contraction coupling in human ventricular myocardium. *J Clin Invest.* 1988;82(5):1592–1605.
52. Ulshöfer R, Bros H, Hauser AE, et al. Preventing axonal sodium overload or mitochondrial calcium uptake protects axonal mitochondria from oxidative stress-induced alterations. *Oxid Med Cell Longev.* 2022;2022:6125711.
53. Oanh NTK, Lee HS, Kim YH, et al. Regulation of nuclear DNA damage response by mitochondrial morphofunctional pathway. *Nucleic Acids Res.* 2022;50(16):9247–9259.